LOCKHEED MARTIN ENERGY RESEARCH LIBRARIES
3 4456 0515881 5

CENTRAL RESEARCH LIBRARY
DOCUMENT COLLECTION

1

ORNL-4104
UC-25 – Metals, Ceramics, and Materials

IRRADIATION BEHAVIOR OF Eu_2O_3–STAINLESS STEEL DISPERSIONS

C. F. Leitten, Jr.
A. E. Richt
R. J. Beaver

OAK RIDGE NATIONAL LABORATORY
CENTRAL RESEARCH LIBRARY
DOCUMENT COLLECTION
LIBRARY LOAN COPY
DO NOT TRANSFER TO ANOTHER PERSON
If you wish someone else to see this document, send in name with document and the library will arrange a loan.
UCN-7969
(3 3-67)

OAK RIDGE NATIONAL LABORATORY
operated by
UNION CARBIDE CORPORATION
for the
U.S. ATOMIC ENERGY COMMISSION

Printed in the United States of America. Available from Clearinghouse for Federal Scientific and Technical Information, National Bureau of Standards, U.S. Department of Commerce, Springfield, Virginia 22151
Price: Printed Copy $3.00; Microfiche $0.65

LEGAL NOTICE

This report was prepared as an account of Government sponsored work. Neither the United States, nor the Commission, nor any person acting on behalf of the Commission:

A. Makes any warranty or representation, expressed or implied, with respect to the accuracy, completeness, or usefulness of the information contained in this report, or that the use of any information, apparatus, method, or process disclosed in this report may not infringe privately owned rights; or

B. Assumes any liabilities with respect to the use of, or for damages resulting from the use of any information, apparatus, method, or process disclosed in this report.

As used in the above, "person acting on behalf of the Commission" includes any employee or contractor of the Commission, or employee of such contractor, to the extent that such employee or contractor of the Commission, or employee of such contractor prepares, disseminates, or provides access to, any information pursuant to his employment or contract with the Commission, or his employment with such contractor.

ORNL-4104

Contract No. W-7405-eng-26

METALS AND CERAMICS DIVISION

IRRADIATION BEHAVIOR OF Eu_2O_3–STAINLESS STEEL DISPERSIONS

C. F. Leitten, Jr., A. E. Richt, and R. J. Beaver

JUNE 1967

OAK RIDGE NATIONAL LABORATORY
Oak Ridge, Tennessee
operated by
UNION CARBIDE CORPORATION
for the
U.S. ATOMIC ENERGY COMMISSION

LOCKHEED MARTIN ENERGY RESEARCH LIBRARIES
3 4456 0515881 5

CONTENTS

Page

Abstract 1
Introduction 1
Background Information 3
Irradiation Test Design 8
Sampling of Irradiated Specimens 10
Specimen Dosimetry and Burnup Analysis 10
Dimensional Changes 12
Microstructural Changes 14
Bonding of the Cladding 14
Microhardness Results 18
Corrosion Tests 18
Conclusions 23
Acknowledgment 24
Appendix A: Details of the Heat Transfer Calculations 27
Appendix B: Irradiation History 33
Appendix C: Calculation of Europium Depletion 37

IRRADIATION BEHAVIOR OF Eu_2O_3–STAINLESS STEEL DISPERSIONS

C. F. Leitten, Jr.,[1] A. E. Richt, and R. J. Beaver

ABSTRACT

Europium has excellent potential in control rods as an absorber of thermal neutrons. It was desired, in the form of Eu_2O_3, for the stainless steel control rods for the Army's SM-1 reactor at Fort Belvoir, Virginia. However, at the time of selection, the use of Eu_2O_3 with stainless steel was questionable because of a reaction with stainless steel during fabrication. Subsequent experiments showed that silicon was responsible for this instability. Acceptable components were made for the SM-1 reactor with stainless steel containing less than 0.03% Si. Irradiation in the ETR verified that these mixtures of Eu_2O_3 with low-silicon stainless steel remained stable through long exposures to thermal neutrons. Mixtures containing 20, 30, and 40 wt % Eu_2O_3 were tested to exposures ranging from 0.7×10^{21} to 4.5×10^{21} neutrons/cm^2 at a temperature estimated to be 150°F. No instabilities or reactions were observed by microstructural examination and dimensional measurement. Europium oxide is prone to attack when exposed to water. Irradiation did not appear to have any effect on this property. Mass spectrographic analyses of the europium after irradiation indicated that the actual burnup of europium was about an order of magnitude less than that predicted by unperturbed neutron flux values or ^{60}Co monitoring.

INTRODUCTION

During the development of neutron absorbers for the control rods of the Army's SM-1 reactor, the limitations in the burnup capability of boron for this application became apparent.[2] Europium in the form of a

---

[1]Present Address: Union Carbide Corporation, Linde Division, Indianapolis, Indiana.

[2]A. E. Richt, C. F. Leitten, Jr., and R. J. Beaver, Postirradiation Evaluation of Stainless Steel Clad Plate Type Specimens Containing 3 wt % Enriched Boron in Iron, ORNL-TM-815 (June 1964).

dispersion of Eu_2O_3 in stainless steel was selected as a replacement for the ^{10}B isotope and in preference to other high neutron-absorbing lanthanides because of its superior burnup characteristics.[3] The europium reaction yields a series of four additional europium isotopes, all of which possess comparatively high neutron-capture cross sections in the energy range of interest. Previous investigations at KAPL indicated that Eu_2O_3 could be readily incorporated in stainless steel by powder metallurgy procedures.[4] However, examination of unclad compacts containing 20 and 30 wt % Eu_2O_3 in stainless steel, which had been irraadiated for two cycles in the MTR, revealed a significant decrease in ductility, structural damage adjacent to the Eu_2O_3 particles, and some volume increase.[4] In our materials development work[5] we proved conclusively that silicon reduced europium oxide with deleterious effects similar to those observed[4] in the KAPL irradiations. Therefore, we attributed the irradiation damage to the concentration of silicon in the stainless steel used by the KAPL investigators, which we believe was sufficient to cause a gross reaction with Eu_2O_3. To conclusively demonstrate the stability of Eu_2O_3 with low-silicon stainless steel, we conducted irradiation tests in the ETR at ambient temperatures for exposures up to 475 full power days at unperturbed thermal neutron fluxes near 1×10^{14} neutrons cm^{-2} sec^{-1}. Our specimens were small composite stainless-steel-clad plates containing 20, 30, or 40 wt % Eu_2O_3 dispersed in stainless steel made from low-silicon iron, nickel, and chromium elemental powders. The Eu_2O_3–stainless steel mixtures were pressed and sintered to high densities and clad with wrought stainless steel by conventional hot roll bonding. Postirradiation evaluation of the effects

---

[3]H. E. Stevens, "Nuclear Requirements for Control Materials," Nucl. Sci. Eng. 4, 373–85 (1958).

[4]W. K. Anderson and D. N. Dunning, "Radiation Damage Resistance of Some Rare Earth Cermets," Nucl. Sci. Eng. 4, 458–66 (1958).

[5]C. F. Leitten, Jr., The Stability of Europium Oxide in Silicon-Bearing Stainless Steel, ORNL-2946 (Aug. 6, 1960).

of reaction between Eu_2O_3 and stainless steel was based primarily on dimensional and microstructural changes. The possible influence of irradiation on the corrosion of the Eu_2O_3–stainless steel mixture was qualitatively assessed. Analyses of the ^{60}Co isotope in the irradiated stainless steel cladding and isotopic analysis of the europium were used as a measure of dosimetry and burnup of the europium.

BACKGROUND INFORMATION

The design of the control rod in the SM-1 reactor is illustrated in Fig. 1. It is composed primarily of two separate segments housed in a stainless steel tube or "basket" of square cross section. The upper segment is the neutron-absorber section, which rests in the active lattice when the rod is fully inserted, while the lower segment is the fuel-bearing section, which resides in the active lattice when the assembly is fully withdrawn. Compartmented rather than integral construction was employed in this instance to eliminate problems of handling extra-long components during fabrication, shipment, and reactor operation. Either or both segments are easily removed by disengagement of the safety lock provided at the upper end of the assembly. The locking cap fixes and firmly holds the components in place during reactor operation. An extension shaft with rack is attached at the lower end of the assembly to make positive connections with the pinion gear box and shock absorber in the bottom of the pressure vessel.

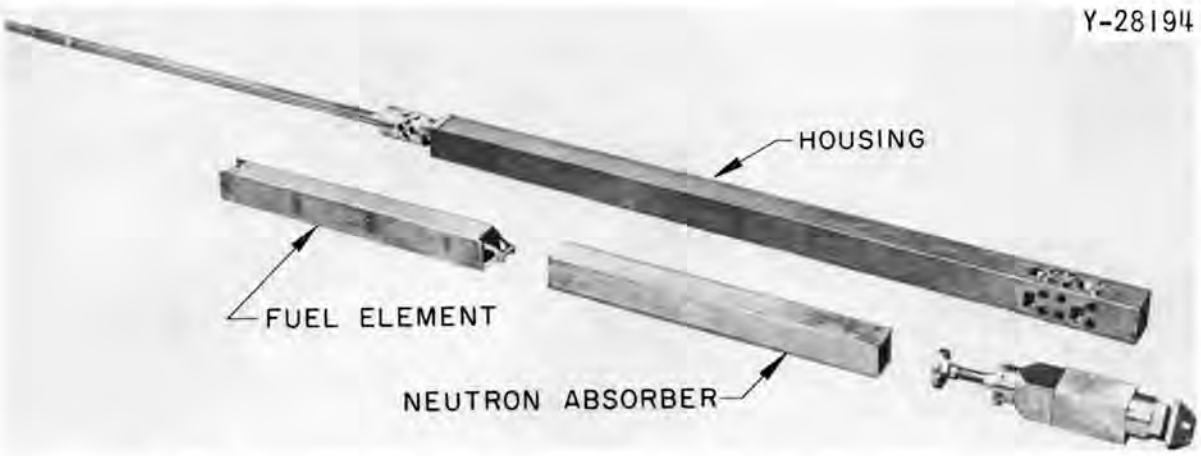

Fig. 1. Component Parts of SM-1 Control Rod Assembly.

The sides of the initial Core-I absorber consisted of composite plates containing 3 wt % enriched ^{10}B dispersed in electrolytic iron as core material and clad with stainless steel. During neutron bombardment ^{10}B undergoes an (n,α) reaction so boron-bearing bodies may swell due to the attendant generation of helium. The miniature Core-I-type stainless-steel-clad specimens exhibited core-cladding separation and swelling after approximately 5% burnup of the ^{10}B atoms in the MTR.[2] We also observed[6] core-cladding separation at the tip ends of the Core I boron-iron absorber sections after 10 Mwyr of service in the SM-1.

Unlike ^{10}B, europium does not yield gaseous products such as helium under irradiation, and thus the damage due to the evolution and expansion of gas with temperature would not be encountered. We, therefore, elected to replace the boron-bearing absorbers with some containing a dispersion of Eu_2O_3 in stainless steel.[7]

Our investigations of the compatibility of Eu_2O_3 with stainless steel and the elements that make up stainless steel showed that silicon reacted with Eu_2O_3; and, in most cases, increases in volume were associated with the reaction.[5] Table 1 summarizes an important phase of this work. The results cited are based on experiments in which dense cylindrical pellets containing 30 wt % Eu_2O_3 in the designated matrix materials were heat treated for 1 1/2 hr at 1250°C in hydrogen at a −62°F dew point. Normally, such pellets shrink when treated in this manner, and the specimen retains its metallic luster. Such was the case for electrolytic iron, carbonyl nickel, electrolytic chromium, and the stainless steel made from these elemental powders. All other matrix materials showed various degrees of instability and indications of reaction, which could be attributed to the silicon content. Figure 2 illustrates the typical effect on the microstructure of the reaction of

---

[6] Army Package Power Reactor Project Ann. Progr. Rept. Jan. 31, 1960, ORNL-2907, pp. 32–37.

[7] C. F. Leitten, Jr., R. J. Beaver, and J. E. Cunningham, Specifications and Fabrication Procedures for Europium-Bearing Absorber Rods for Reactivity Control in Core II of SM-1, ORNL-2733 (July 29, 1959).

Table 1. Effect of Silicon on the Stability of Eu_2O_3 in Various Matrix Materials[a]

Matrix Material	Silicon Content	Weight Loss (g)	Volume Change (%)	Specimen Appearance
Type 304B stainless steel	2.34 wt %	0.0038	+6.30	Covered with yellow-green film
	2.34 wt %	0.0041	+6.89	Covered with yellow-green film
	2.34 wt %	0.0033	+6.58	Covered with yellow-green film
Type 347B stainless steel	2.08 wt %	0.0050	+5.35	Covered with yellow-green film
	2.08 wt %	0.0078	+3.41	Covered with yellow-green film
	2.08 wt %	0.0073	+3.53	Covered with yellow-green film
	2.08 wt %	0.0071	+3.53	Covered with yellow-green film
Type 304L stainless steel	0.11 wt %	0.0051	−4.22	Lightly covered with yellow-green film
	0.11 wt %	0.0064	−3.89	Lightly covered with yellow-green film
	0.11 wt %	0.0067	−3.12	Lightly covered with yellow-green film
	0.11 wt %	0.0066	−3.38	Lightly covered with yellow-green film
Electrolytic iron	< 10 ppm	0.0085	−2.05	Metallic
	< 10 ppm	0.0090	−2.13	Metallic
Carbonyl nickel	< 10 ppm	0.0050	−14.15	Metallic
	< 10 ppm	0.0061	−13.89	Metallic
	< 10 ppm	0.0058	−14.53	Metallic
Electrolytic chromium	28 ppm	0.0035	−2.69	Metallic
	28 ppm	0.0039	−2.34	Metallic
Type II electrolytic chromium	0.12 wt %	0.0040	+1.72	Covered with yellow-green film
	0.12 wt %	0.0035	+2.02	Covered with yellow-green film

Table 1 (continued)

Matrix Material	Silicon Content	Weight Loss (g)	Volume Change (%)	Specimen Appearance
Type III electrolytic chromium	58 ppm	0.0036	−4.97	Very slightly covered with yellow-green film
	58 ppm	0.0030	−5.36	Very slightly covered with yellow-green film
	58 ppm	0.0040	−2.08	Very slightly covered with yellow-green film
Elemental Fe-Ni-type I-Cr		0.0059	0.00	Metallic
		0.0059	+0.07	Metallic
Elemental Fe-Ni-type II-Cr		0.0061	+2.27	Covered with yellow-green film
		0.0057	+2.13	Covered with yellow-green film
Elemental Fe-Ni-type III-Cr		0.0058	−0.34	Metallic
		0.0053	+0.11	Metallic
Type 304 stainless steel	0.22 wt %		+2.60	Slightly covered with yellow-green film
	0.22 wt %		+2.80	Slightly covered with yellow-green film
	0.22 wt %		+2.93	Slightly covered with yellow-green film
	0.22 wt %		+2.76	Slightly covered with yellow-green film

[a]The europium oxide used had been conditioned at 1700 °C for 3 hr under hydrogen.

Eu_2O_3 with type 347B stainless steel, whose silicon concentration is 2.08%. Each stainless steel particle appears to be surrounded by a reaction product. The formation of a second phase in the oxide particle is also evident. These results show that to completely avoid a reaction between Eu_2O_3 and stainless steel, the silicon content should be limited to less

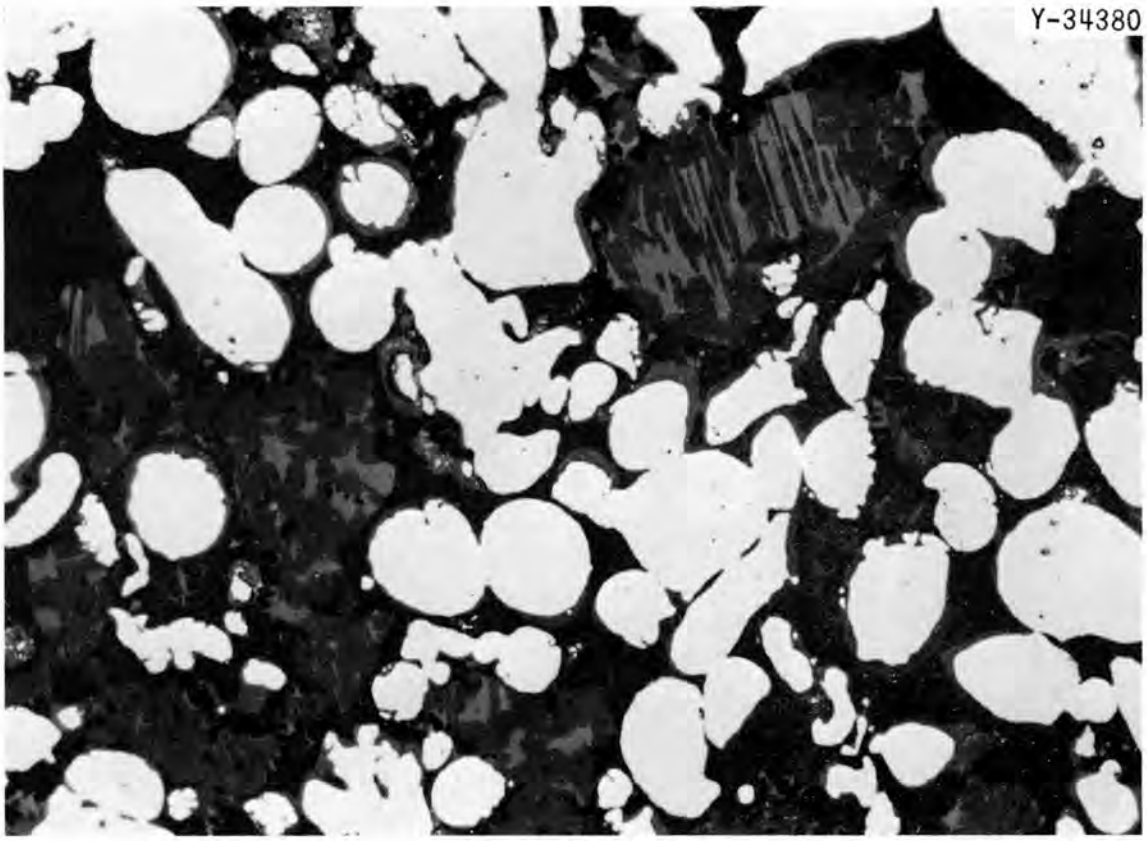

Fig. 2. Microstructure of a 30% Eu_2O_3 Dispersion in Type 347B Stainless Steel Heat Treated at 1230°C for 1 1/2 hr Under Hydrogen. As polished. 500×.

than 0.0015%. Other work[8] indicated, however, that no unusual difficulty would be expected if the silicon content reached 0.03 wt %. Similar compatibility studies on gadolinium and samarium oxide dispersed in commercial stainless steel did not show a dependence on silicon content.

Parallelling our work, KAPL was also investigating the use of lanthanide oxides for dispersions in nuclear control for pressurized water reactors. Cursory irradiation tests were performed on stainless-steel-base cermets containing various amounts of lanthanide oxides in the MTR.[9]

---

[8]C. F. Leitten, Jr., The Stability of Europium Oxide in Silicon-Bearing Stainless Steel, ORNL-2946 (Aug. 6, 1960).

[9]W. K. Anderson and D. N. Dunning, "Radiation Damage Resistance of Some Rare Earth Cermets," Nucl. Sci. Eng. 4, 458–66 (1958).

Postirradiation examination of these cermets indicated that Gd_2O_3-bearing cermets were not damaged as a result of irradiation. However, severe embrittlement and some growth was observed in the tests containing Eu_2O_3. Because of the similarity of these effects with our observations of the chemical compatibility of europium oxide, we suspected that under irradiation, even at low temperatures, the cause of damage was associated with chemical interaction and not irradiation damage per se. We, therefore, set out to demonstrate that Eu_2O_3 is stable in a low-silicon (0.03 wt % max) stainless steel. The design of our irradiation test and facilities used was similar to that we previously used for iron-boron specimens.[10]

IRRADIATION TEST DESIGN

The miniature test specimens were irradiated in various beryllium reflector positions in the Engineering Test Reactor. The unperturbed thermal neutron flux in these positions was estimated to be about 1×10^{14} neutrons cm^{-2} sec^{-1}. The design is relatively simple; specimens are encased in "leaky rabbits," 7 1/2 in. long, which are stacked in a tubular housing that fits the hole through the beryllium reflector. A specimen in a "leaky rabbit" ready for insertion is illustrated in Fig. 3. The specimens are cooled by the process water at a temperature

[10] A. E. Richt, C. F. Leitten, Jr., and R. J. Beaver, Postirradiation Evaluation of Stainless Steel Clad Plate Type Specimens Containing 3 wt % Enriched Boron in Iron, ORNL-TM-815 (June 1964).

Fig. 3. Composite Stainless Steel–Eu_2O_3 Specimen in Irradiation Test Capsule.

estimated to be 115 °F. The calculated maximum center line temperature of the specimen was 170 °F; details of the calculations are included in Appendix A.

We planned to evaluate the influence of the Eu_2O_3 concentration and the tenure under irradiation on the stability of Eu_2O_3 dispersed in low-silicon stainless steel. The concentrations we chose were 20, 30, and 40 wt % Eu_2O_3, which we consider an acceptable symmetry about the 36 wt % eventually specified for the europium oxide–stainless steel absorber now operating in the Army's stationary medium power reactors. Our intentions were to expose the specimens to 7×10^{20}, 14×10^{20}, 28×10^{20}, and 45×10^{20} neutrons/cm^2. Twelve specimens were required. Pertinent design details on these specimens are listed in Table 2. The specimens

Table 2. Pertinent Data on Irradiation Test Specimens

Nominal Dimensions	
Overall,	6.0 in. long, 1.00 in. wide, 0.156 in. thick
Core Section,	5.0 in. long, 0.55 in. wide,[a] 0.090 in. thick
Materials	
Cladding,	wrought type 304L stainless steel
Framing,	wrought type 304L stainless steel
Matrix,	stainless steel prepared from the elemental powders
Particle size, μ	Fe, <10; Ni, <10; Cr, <10
Concentration, wt %	Fe, 71; Ni, 11; Cr, 18
Silicon content, ppm	Fe, <10; Ni, <10; Cr, 28
Dispersoid, monoclinic Eu_2O_3 conditioned by firing at 1700 °C in hydrogen for 3 hr[b]	

[a]Maximum.

[b]Specific manufacturing details given in report by C. F. Leitten, Jr., R. J. Beaver, and J. E. Cunningham, Specifications and Fabrication Procedures for Europium-Bearing Absorber Rods for Reactivity Control in Core II of SM-1, ORNL-2733 (July 29, 1959).

were prepared by procedures that we established[11] for manufacturing hot-rolled composite plates for the SM-1 absorber sections. Of course, the irradiation test samples were smaller in length and width. In addition, the rolled core was elliptical. For convenience, we used a Eu_2O_3—stainless steel compact that was a 1/2-in.-diam right circular cylinder, and the rolling process caused the elliptical shape in the final product. Previous experience[10] indicated that the major dimensional change in specimens of this design would be in thickness. For comparative purposes we designed the irradiation test specimens as thick as specified for the full-size SM-1 absorber plate.

SAMPLING OF IRRADIATED SPECIMENS

The sampling plan for the irradiated specimens is illustrated in Fig. 4. Four sections were removed from each specimen by sawing through at the locations shown with a water-cooled abrasive cut-off wheel. You will note that the dosimetry sample was cut from the "inactive" stainless steel end; the samples for analysis of the europium burnup, examination of microstructural changes, and postirradiation corrosion testing were taken from the midsection of the specimen.

SPECIMEN DOSIMETRY AND BURNUP ANALYSIS

The calculation of burnup in neutron absorber materials from ununperturbed thermal-neutron dose values is complicated both by local perturbation of the flux in the vicinity of such specimens and by the high degree of self-shielding within the absorber material proper. Except for the boron-bearing absorber materials, analytical determination of the extent of poison burnup is also an expensive and time-consuming operation. Consequently, most of the previous irradiation damage studies on neutron absorber materials have reported specimen exexposures simply in terms of the unperturbed thermal-neutron dose.

---

[11]C. F. Leitten, Jr., R. J. Beaver, and J. E. Cunningham, Specifications and Fabrication Procedures for Europium-Bearing Absorber Rods for Reactivity Control in Core II of SM-1, ORNL-2733 (July 29, 1959).

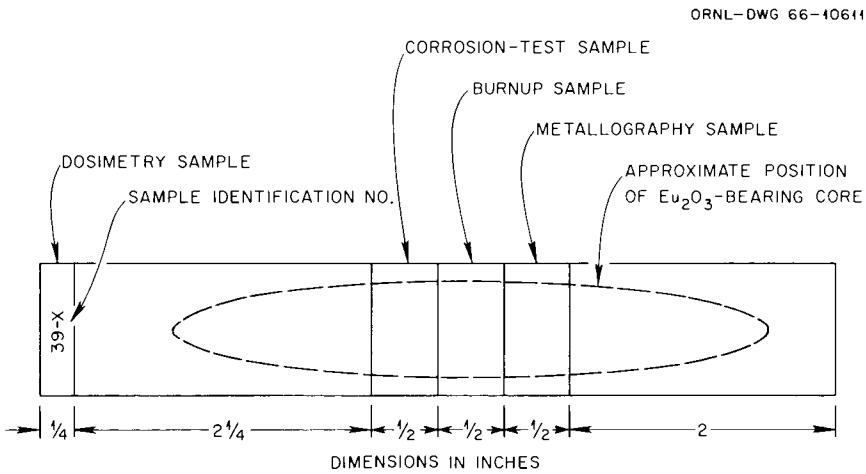

Fig. 4. Sectioning Diagram for Eu_2O_3–Stainless Steel Irradiation Test Specimens.

A second complication arises when one attempts to compare the irradiation performance of different type absorber materials. For example, how does one compare the performance of a 1 wt % ^{10}B–stainless steel alloy with that of a hafnium, silver-indium-cadmium, or Eu_2O_3–stainless steel absorber material? If the geometry of the absorber is identical, the only valid comparative expression of burnup in the different absorber materials is the number of neutrons that have been absorbed per unit volume of the absorber material.

For these reasons, the exposures received by specimens in this irradiation test program are reported in two different terms: (1) the unperturbed thermal-neutron dose, to allow a crude comparison with previous irradiation damage studies, and (2) neutrons absorbed per cubic centimeter of total core material.

A section from the stainless steel end of each test specimen was used as a specimen neutron dosimeter. These sections were analyzed radiochemically to determine the quantity of ^{60}Co formed during irradiation. These data were used to calculate the integrated thermal-neutron flux received by each specimen. As shown in Table 3, the dosimetry-derived values were generally found to be approximately 20% lower than the ETR-quoted unperturbed thermal-neutron doses. This was not unexpected, since the thermal-neutron flux in the test facilities should be depressed somewhat by the presence of the highly absorbing test specimens.

Table 3. Comparison of Dosimetry Results with Burnup Results of Europium in Eu_2O_3–Stainless Steel Specimens

Specimen	Eu_2O_3 (wt %)	Specimen Dose, neutrons/cm^2		Europium Burnup (neutrons/cm^3) Neutrons Absorbed Per	
		From ETR Estimates[a]	From ^{60}Co Activation	Original Europium Atom	Cubic Centimeter of Core
		$\times 10^{20}$	$\times 10^{20}$		$\times 10^{21}$
39-1	20	7.0	3.7	0.13[b]	0.6[b]
39-2	20	12.1	10.3	0.19	0.9
39-3	20	28.1	21.9	0.55	2.6
39-4	20	45.0	52.1	0.88	4.1
39-5	30	7.6	6.0	0.13[b]	0.9[b]
39-6	30	14.6	12.8	0.25[b]	1.8[b]
39-7	30	27.9	19.3	0.49[b]	3.5[b]
39-8	30	45.0		0.80[b]	5.7[b]
39-9	40	7.2	4.9	0.11[b]	1.0[b]
39-10	40	14.8	11.7	0.26	2.4
39-11	40	28.7	24.2	0.43	4.0
39-12	40	42.8	34.9	0.69	6.4

[a]Unperturbed thermal-neutron values calculated from irradiation data shown in Appendix B.

[b]Interpolated values from data presented in Appendix C.

Sections from six of the absorber plates (39-2, 39-3, 39-4, 39-10, 39-11, and 39-12) were analyzed mass spectrographically to determine the europium isotopic composition. The isotopic data were used to determine the europium burnup in each of the six specimens. The methods used in calculation of burnup from the isotopic ratios are described in Appendix C. Results of the burnup determinations are also shown in Table 3.

DIMENSIONAL CHANGES

Pre- and postirradiation thickness and width were measured with a remotely operated dial-gage micrometer capable of an accuracy of ±0.0001 in. Similarly, length was measured with a vernier micrometer with an accuracy of ±0.001 in. The results in Table 4 show that the samples maintained excellent dimensional stability at burnup as high as

Table 4. Comparison of Pre- and Postirradiation Dimensional Measurements on Eu_2O_3–Stainless Steel Neutron Absorber Specimens

Specimen Number	Eu_2O_3 Loading (wt %)	Specimen Burnup (neutrons absorbed per cm^3)	Specimen Thickness (in.)[a]			Specimen Width (in.)[a]			Specimen Length (in.)[b]		
			Preirradiation	Postirradiation	Change	Preirradiation	Postirradiation	Change	Preirradiation	Postirradiation	Change
		($\times 10^{21}$)									
39-1	20	0.6	0.1543	0.1542	−0.0001	0.9834	0.9837	+0.0003	6.001	6.002	+0.001
39-2	20	0.9	0.1546	0.1546	0.0000	0.9834	0.9834	0.0000	6.002	6.004	+0.002
39-3	20	2.6	0.1574	0.1577	+0.0003	0.9813	0.9810	−0.0003	6.001	6.001	0.000
39-4	20	4.1	0.1578	0.1583	+0.0005	0.9831	0.9828	−0.0003	6.000	6.001	+0.001
39-5	30	0.9	0.1581	0.1580	−0.0001	0.9838	0.9840	+0.0002	6.000	6.001	+0.001
39-6	30	1.8	0.1580	0.1583	+0.0003	0.9843	0.9846	+0.0003	6.001	6.001	0.000
39-7	30	3.5	0.1592	0.1594	+0.0002	0.9831	0.9836	+0.0005	6.001	6.002	+0.001
39-8	30	5.7	0.1591	0.1593	+0.0002	0.9838	0.9840	+0.0002	6.000	6.001	+0.001
39-9	40	1.0	0.1529	0.1529	0.0000	0.9840	0.9843	+0.0003	6.000	6.000	0.000
39-10	40	2.4	0.1530	0.1529	−0.0001	0.9839	0.9838	−0.0001	6.000	6.001	+0.001
39-11	40	4.0	0.1557	0.1560	+0.0003	0.9846	0.9850	+0.0004	6.002	6.002	0.000
39-12	40	6.4	0.1559	0.1562	+0.0003	0.9834	0.9835	+0.0001	6.002	6.001	−0.001

[a]Average of 11 measurements.

[b]Average of three measurements.

6.4×10^{21} absorptions/cm^3. This excellent performance was also observed in the dimensional examination of a full-size absorber section, which had operated through 10 Mwyr of service in the active lattice of the SM-1 reactor.[12]

MICROSTRUCTURAL CHANGES

Each specimen was examined in detail for evidence of irradiation-induced damage to the microstructure of the Eu_2O_3–stainless steel mixture. Representative portions of the microstructures in the as-polished condition are illustrated in Fig. 5 for the 20, 30, and 40 wt % Eu_2O_3–stainless steel specimens at europium burnups ranging from 4.9 to 6.1×10^{21} absorptions/cm^3. No evidence of interaction exists, and comparison with the unirradiated material shows no significant differences. It is also important to note the integrity of the matrix in these specimens. No evidence of matrix cracking or particle-matrix separation was observed. Figure 6 compares at high magnification the microstructure of a 20 wt % Eu_2O_3 dispersion exposed to 4.9×10^{21} neutrons/cm^3 with its unirradiated counterpart. Again, no evidence of interaction between Eu_2O_3 and stainless steel exists. A most interesting feature, however, is the appearance of twinning in the Eu_2O_3 particles. The ability of Eu_2O_3 to deform plastically has also been observed in pressed and sintered pellets.[13]

BONDING OF THE CLADDING

While examining sections from the various plates metallographically, we included a careful inspection of the bond between the Eu_2O_3–stainless

---

[12] A. E. Richt, Interim Postirradiation Examination of a Europium-Bearing Control Rod from the Stationary Medium Power Reactor, ORNL-TM-1407 (March 1966).

[13] G. L. Ploetz et al., "Sintering Characteristics of Rare-Earth Oxides," J. Am. Ceram. Soc. 41, 551–54 (December 1958).

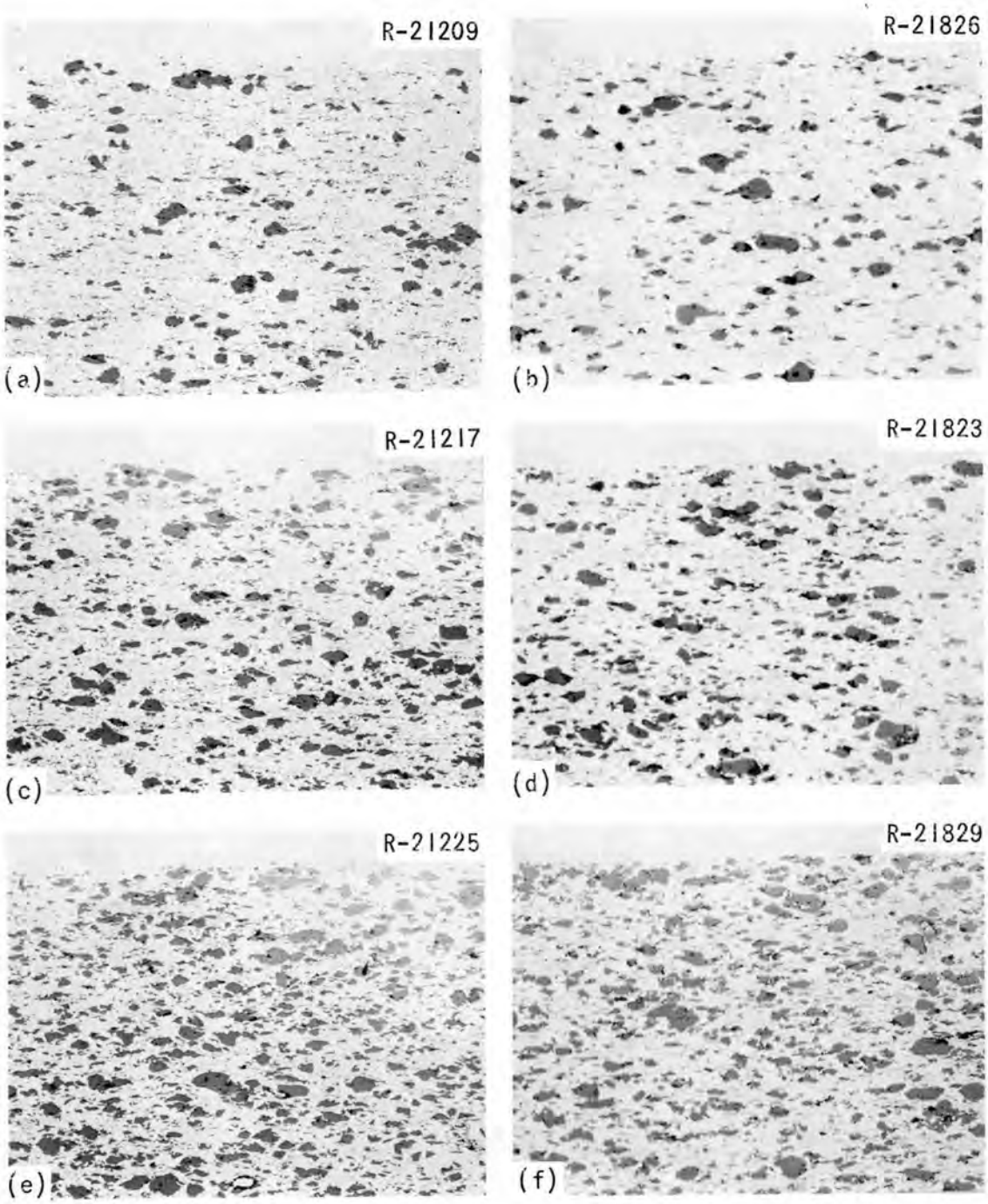

Fig. 5. Typical Microstructures of Eu_2O_3 Dispersion Absorber Plates. As polished. 100×. Note near the top of each photomicrograph the bonded interface between the type 304L stainless steel cladding and the dispersion core. (a) 20% Eu_2O_3 unirradiated. (b) 20% Eu_2O_3 after 4.9×10^{21} neutron absorptions/cm^3. (c) 30% Eu_2O_3 unirradiated. (d) 30% Eu_2O_3 after 5.5×10^{21} neutron absorptions/cm^3 (e) 40% Eu_2O_3 unirradiated. (f) 40% Eu_2O_3 after 6.1×10^{21} neutron absorptions/cm^3.

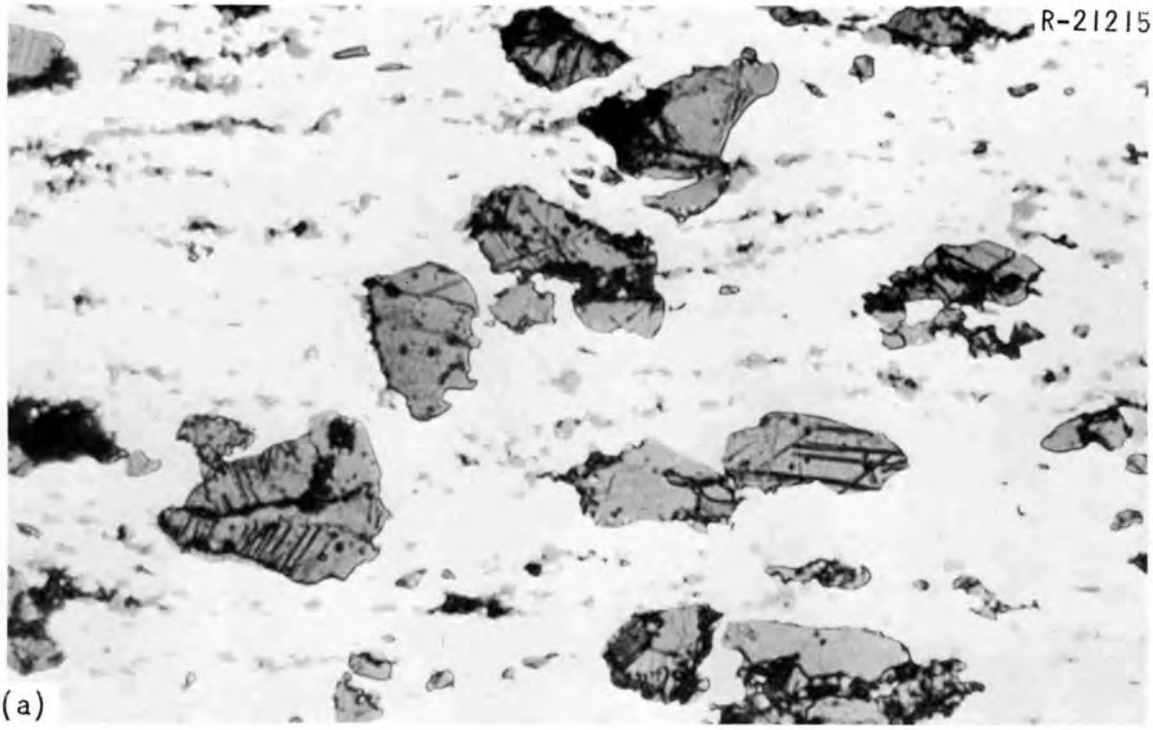

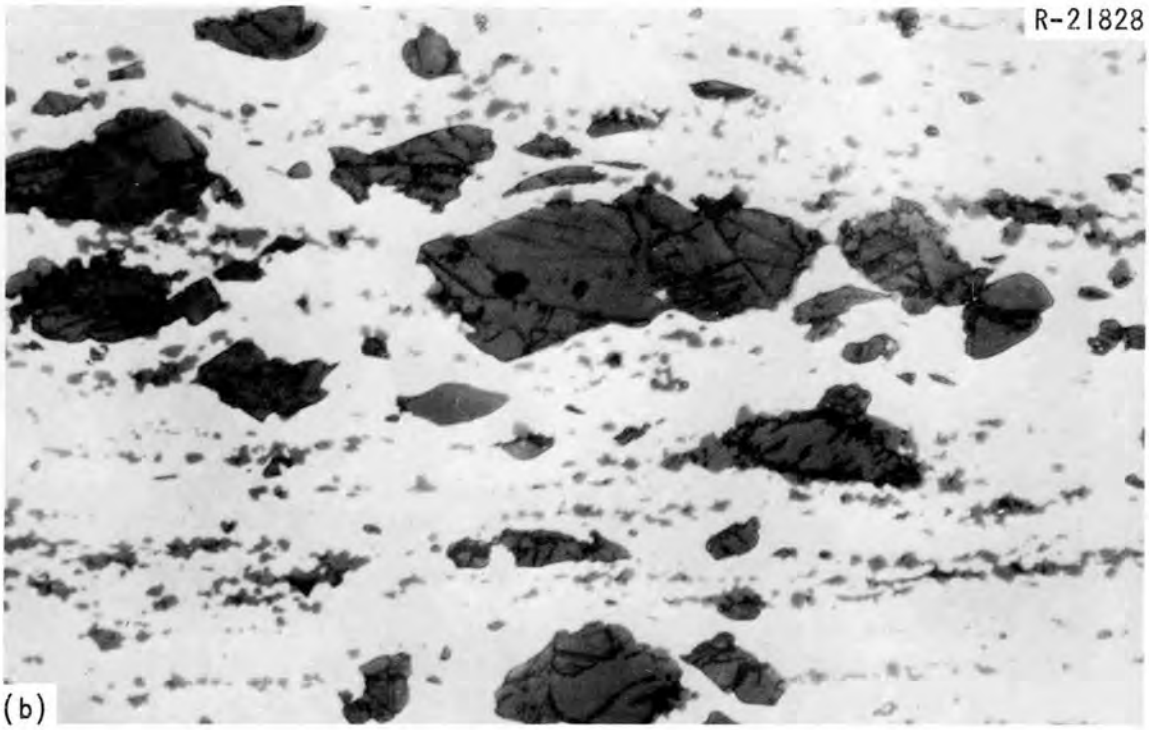

Fig. 6. Microstructure of Eu_2O_3 Particles in Stainless Steel–20% Eu_2O_3. (a) Unirradiated. (b) After absorbing 4.7×10^{21} neutrons/cm^3. Etchant: 10% HNO_3–10% H_2O_2–80% H_2O. 750×.

steel section and the stainless steel cladding. In no case did we find any indication that irradiation caused localized bond failures. A comparison of the core-cladding bond before and after the longest irradiation exposure in this program is illustrated in Fig. 7. We feel that this is good evidence of the integrity that results from the hot roll bonding process we developed for the SM-1 absorber plates.[14]

---

[14]C. F. Leitten, Jr., R. J. Beaver, and J. E. Cunningham, Specifications and Fabrication Procedures for Europium-Bearing Absorber Rods for Reactivity Control in Core II of SM-1, ORNL-2733 (July 29, 1959).

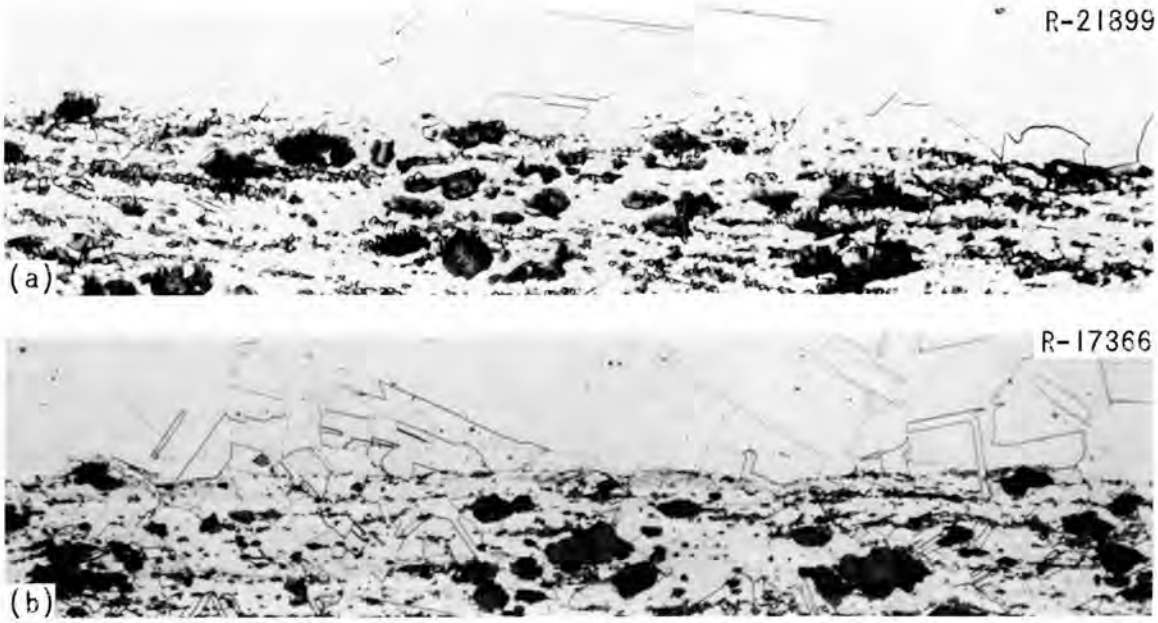

Fig. 7. Typical Microstructure of Interface Between Cladding and 40 wt % Eu_2O_3–Stainless Steel Dispersion Before and After Irradiation. (a) Unirradiated. (b) After 6.1×10^{21} neutron absorptions/cm^3. Etchant, Glycerol Regia. 250×

MICROHARDNESS RESULTS

The results of microhardness tests of the europium-bearing core and the cladding are listed in Table 5. Comparisons between unirradiated and irradiated specimens generally show increases in hardness ranging from 30 to 50%, and the more pronounced effect is the hardening of the cladding. We feel that these hardness increases reflect the influence of fast neutrons (> 1 Mev). We estimate this exposure to be in the order of 5×10^{19} neutrons/cm^2.

CORROSION TESTS

We were aware that Eu_2O_3 is hygroscopic and that dispersions of Eu_2O_3 in stainless steel are prone to deteriorate when exposed to water.[15] We were curious, however, about the effect that neutron irradiation might have on this property of Eu_2O_3 and exposed the edges of samples of both unirradiated and irradiated specimens for 88 hr in static water at 570°F and 1200 psi. These conditions were selected because they were a good approximation of the SM-1 water temperature and pressure.

The effect of these tests is dramatically illustrated in Figs. 8 through 11. Pertinent dimensional and weight-change data are listed in Table 6. In all cases, water has permeated the material and has hydrolyzed the Eu_2O_3 to promote a volume increase. This swelling stresses the surrounding matrix material, causing cracks and then exfoliations in the weaker regions. Swelling is pronounced in the 30 and 40 wt % mixtures. Attack on the 20 wt % dispersion seems to be less by an order of magnitude. A rather interesting observation made in these static corrosion studies was that the europium content in the water did not exceed the detectable limits of analysis. As shown in Fig. 11 the Eu_2O_3 particles appear to remain in place at the surface of the sample consistent with the absence of europium in the static test water.

---

[15]R. A. McNees and R. A. Potter, "Europium Oxide Studies," Army Reactors Program Progress Report, ORNL-3231, pp. 16–22 (Jan. 31, 1962).

Table 5. Pre- and Postirradiation Hardness of Stainless-Steel-Clad Dispersions of Eu_2O_3 in Stainless Steel

Specimen	Eu_2O_3 (wt %)	Burnup (absorptions/cm^3)	Diamond Pyramid Hardness – 2-kg Load					
			Cladding[a]		Core Edge		Core Center	
			Range	Average[b]	Range	Average[b]	Range	Average[b]
2	20	Unirradiated	142–149	146	169–181	175	169–181	175
39-4	20	4.1×10^{21}	210–230	222	266–274	271	266–274	261
3	30	Unirradiated	139–155	149	213–232	218	207–215	211
39-8	30	5.7×10^{21}	208–221	214	258–272	266	271–280	274
4	40	Unirradiated	141–151	146	179–197	188	179–197	188
39-12	40	6.4×10^{21}	227–239	232	246–261	252	238–254	249

[a]Type 304L stainless steel.

[b]Average of eight measurements.

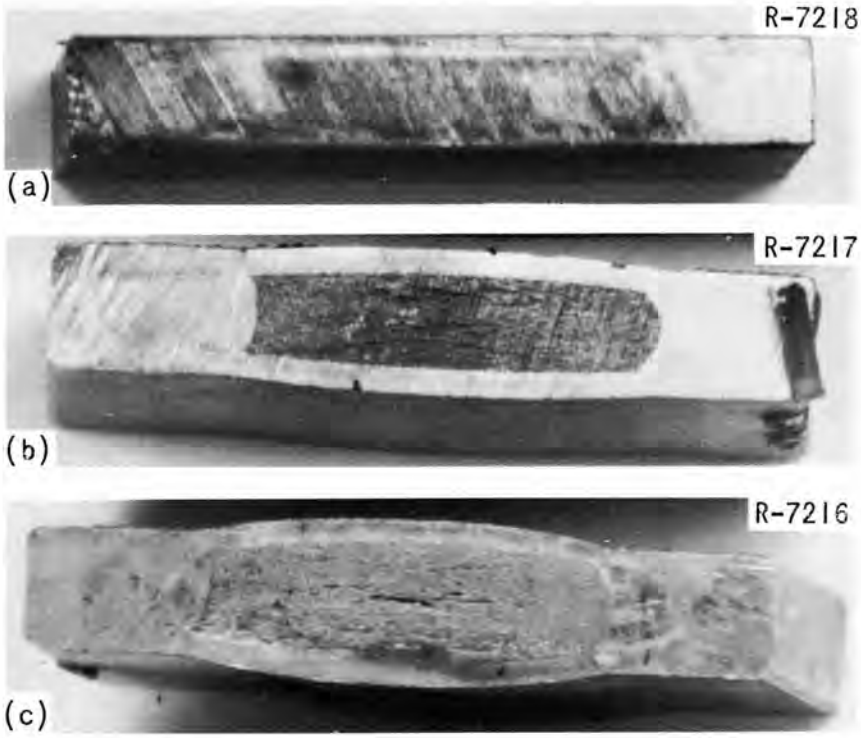

Fig. 8. Overall Appearance of Samples from Irradiated Eu_2O_3–Stainless Steel Specimens After Testing in Water at 570°F and 1200 psi. (a) 20 wt % Eu_2O_3–stainless steel. (b) 30 wt % Eu_2O_3–stainless steel. (c) 40 wt % Eu_2O_3–stainless steel. 4×.

The differences in attack on the 20 wt % Eu_2O_3 mixture compared to the other two dispersions are worth a comment. We feel that this marked difference stems from protection by the stainless steel surrounding the Eu_2O_3 particles. The larger the surface-to-volume ratio of the Eu_2O_3 and the higher the concentration of the Eu_2O_3, the greater the potential for water to reach the Eu_2O_3. In our experiments, the concentration effect is the major factor. Improvements would be anticipated, for example, in the 30 to 40 wt % concentrations if spheroidal particles of somewhat larger size fraction could be used.

These corrosion tests vividly illustrate the chief disadvantage of Eu_2O_3 for water-cooled systems. Therefore, we recommend a substantial thickness of cladding on such a Eu_2O_3-bearing component and that the cladding be metallurgically bonded to the core and nondestructively inspected for bond integrity. In the case of the SM-1 absorber plates, the cladding is specified as 0.032 in. thick and is bonded to the core by a hot-rolling process.

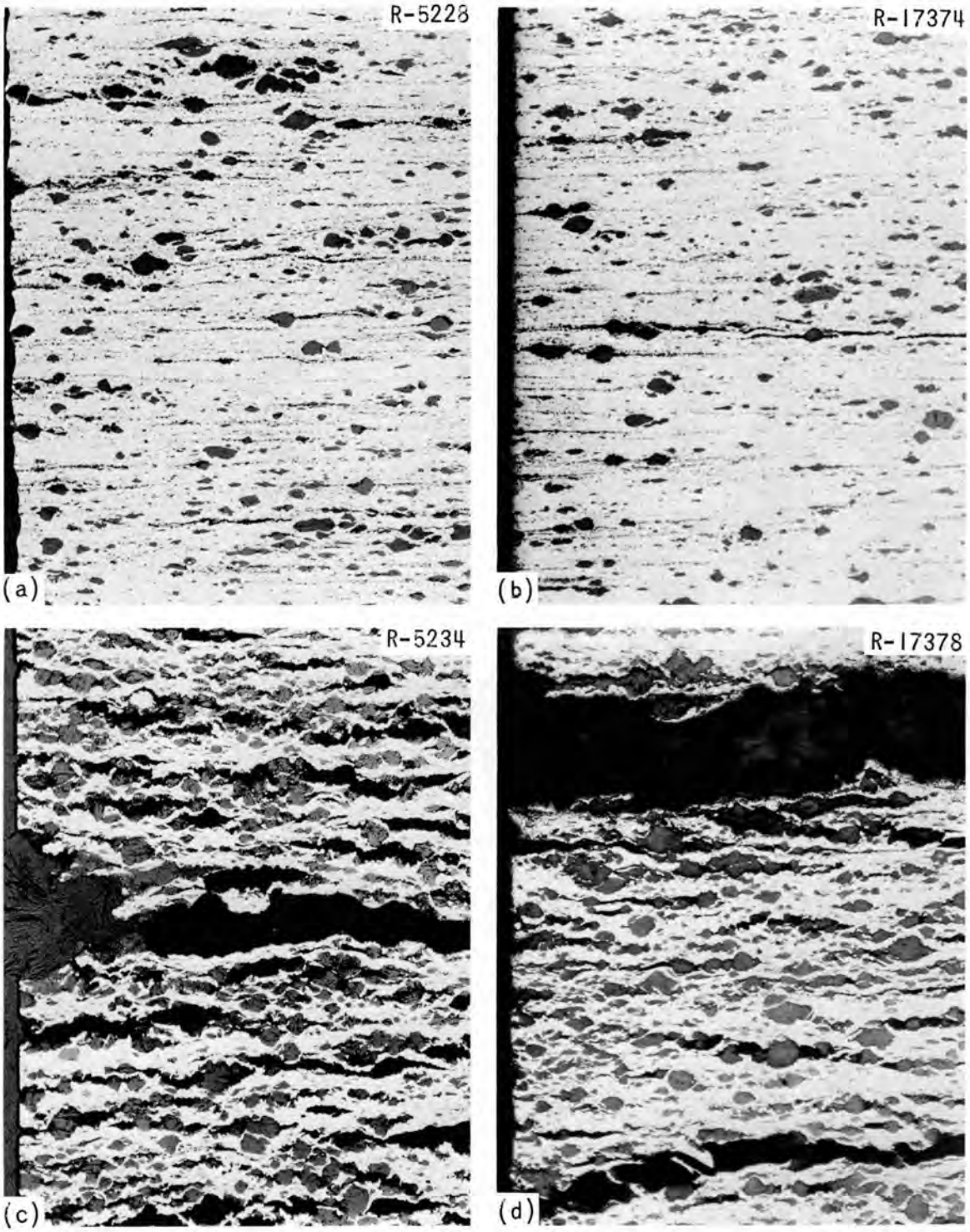

Fig. 9. Typical Microstructures of Eu_2O_3–Stainless Steel After 88-hr Exposure in Water at 570°F and 1200 psi. As polished. 100×. (a) Unirradiated 20% Eu_2O_3. (b) Irradiated 20% Eu_2O_3. (c) Unirradiated 40% Eu_2O_3. (d) Irradiated 40% Eu_2O_3.

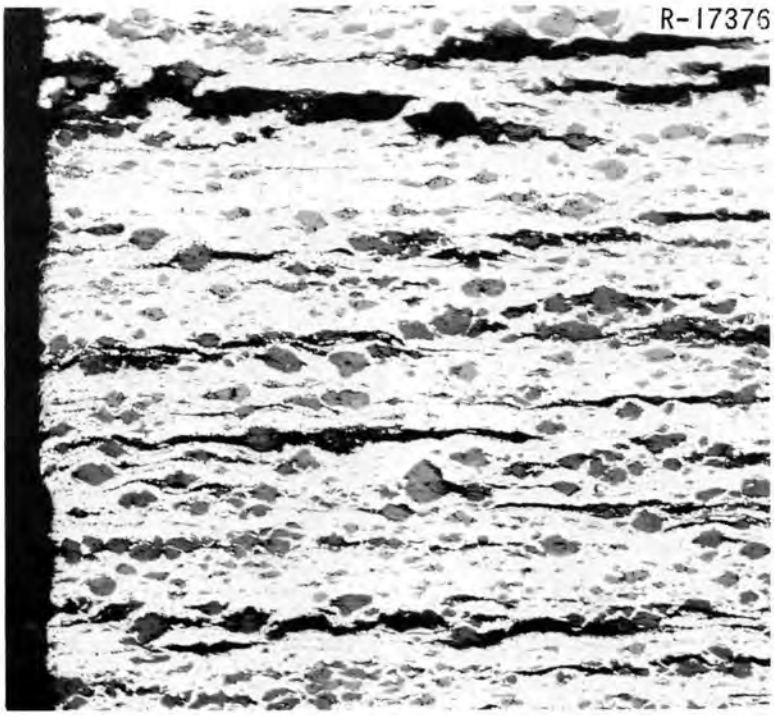

Fig. 10. Typical Microstructure of 30 wt % Eu_2O_3–Stainless Steel After Testing in Water at 570 °F and 1200 psi for 88 hr. 100×.

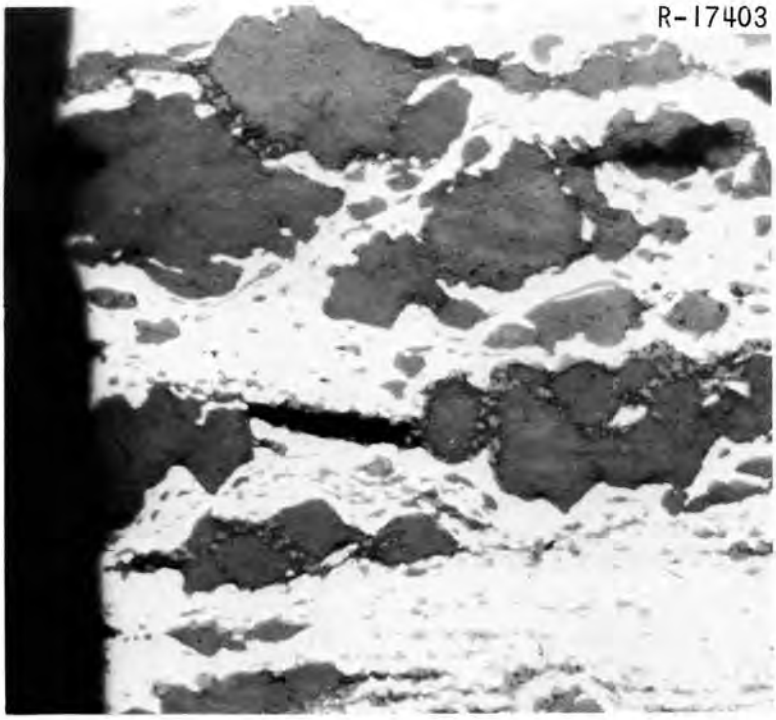

Fig. 11. Exposed Edge of an Irradiated 40% Eu_2O_3–Stainless Steel Dispersion After Exposure to Water at 570 °F. As polished. 500×.

Table 6. Corrosion of Eu_2O_3–Stainless Steel Dispersions in Water at 570°F and 1200 psi[a]

Specimen	Eu_2O_3 (wt %)	Burnup (absorptions/ cm^3)	Weight Gain (%)	Thickness Increase (%)
		$\times 10^{21}$		
2	20	Unirradiated	0.04	0.9
39-1	20	0.6	0.01	0.8
39-2	20	0.9	0.05	2.5
39-3	20	2.6	0.07	0.7
39-4	20	4.0	0.04	0.7
39-5	30	0.9	0.41	13.3
39-6	30	1.8	0.62	15.4
39-7	30	3.5	0.71	11.3
39-8	30	5.7	0.61	12.0
4	40	Unirradiated	1.53	27.3
39-9	40	1.0	0.24	34.0
39-10	40	2.4	1.58	30.5
39-11	40	4.0	1.51	31.3
39-12	40	6.4	1.60	29.5

[a]Samples clad with stainless steel except at ends.

CONCLUSIONS

On the basis of results obtained from postirradiation examination of the stainless-steel-clad specimens containing 20 to 40 wt % Eu_2O_3 with exposures to thermal neutrons as high as 4.5×10^{21} neutrons/cm^2, the following conclusions can be drawn.

1. Metallographic examination shows that no discernable chemical reaction occurs between Eu_2O_3 and an 0.03% Si stainless steel during long exposure to neutrons.

2. Length, width, and thickness measurements show that fabricated dispersions of up to 40 wt % Eu_2O_3 in stainless steel are dimensionally stable under irradiation. This is further evidence that, if the silicon content of materials mixed with Eu_2O_3 is low, no deleterious irradiation damage effects occur.

3. Metallographic examination of the bonding between the Eu_2O_3–stainless steel mixture and the stainless steel cladding shows no

deterioration by irradiation. This evidence supports the fabrication practices established for manufacturing the SM-1 absorber plates with the hot-rolling process.

4. On the basis of metallographic examination and sample weight and thickness changes no evidence was observed that showed that irradiation changes the corrosion characteristics of Eu_2O_3. This compound is prone to hydrolysis and must be protected by a corrosion-resistant cladding for water reactor application.

5. Mass spectrographic techniques can be used to give an accurate measure of the burnup of europium and overcome some of the limitations associated with ^{60}Co monitoring.

ACKNOWLEDGMENT

The authors wish to express their appreciation for the help and cooperation of J. R. Sites and E. I. Wyatt in providing the isotopic and radiochemical analyses, respectively; E. D. Sims in assisting in the metallographic examination; the Reports Office in the preparation of this report. We also wish to thank S. Peterson for his editorial assistance.

Appendix A

Details of the Heat Transfer Calculations

Details of the Heat Transfer Calculations

Surface Temperature

The surface temperature as a result of gamma heating can be calculated, assuming[16] a water flow velocity of 8.7 ft/sec and a gamma heating rate of 10 w/g and using the following expression:

$$Q/A_s = h\Delta T \quad h(T_0 - T_1) \ , \tag{1}$$

where:

Q = heat generation (Btu/hr),

A_s = total surface area of the core (ft^2),

h = heat transfer coefficient of the coolant (Btu $hr^{-1}ft^{-2}{}^\circ F^{-1}$),

ΔT = the temperature difference between the plate surface and the coolant; $\Delta T = T_1 - T_0$, where T_1 = plate surface temperature, T_0 = bulk coolant temperature, assumed to be 115°F.

The heat-transfer coefficient (h) is obtained from the modified Colburn equation:

$$h(D_e/K) = 0.023(D_e V\rho/\mu)_f^{0.8}(C_p\mu/K)_f^{0.3} \ , \tag{2}$$

with all water properties evaluated at the film temperature,

where:

K = thermal conductivity of the film water (Btu $hr^{-1}ft^{-1}{}^\circ F^{-1}$),

ρ = density of coolant (lb/ft^3),

μ = viscosity of the film water (lb $sec^{-1}ft^{-1}$ or lb $hr^{-1}ft^{-1}$),

D_e = equivalent diameter of the channel (ft),

C_p = specific heat of the film water (Btu $lb^{-1}{}^\circ F^{-1}$).

The quantity of heat generated in the miniature plate can be found using an average sample weight of 120 g:

---

[16]Personal communication with R. R. O'Conner, Project Engineer, MTR, March, 1959.

$$120 \text{ g} \times 10 \text{ w/g} = 1.2 \times 10^3 \text{ w}$$

or

$$1.2 \times 10^3 \text{ w} \times 3.413 = 4.10 \times 10^3 \text{ Btu/hr.}$$

Assuming that the plate is nominally 0.983 in. wide × 6 in. long, then the total surface area is:

$$A_s = \frac{2 \times 6 \times 0.983}{144} = 0.0819 \text{ ft}^3 \quad . \tag{3}$$

Thus, the total gamma heat generated per total surface area (thermal flux) is:

$$\frac{Q}{A_s} = \frac{4.10 \times 10^3}{0.0819} = 5.01 \times 10^4 \text{ Btu hr}^{-1} \text{ ft}^{-2} \quad . \tag{4}$$

The equivalent diameter of the water channel in which the specimen is mounted can be calculated as follows:

$$D_e = 4A/P \quad , \tag{5}$$

where:

A = cross sectional area of the channel,

P = total surface perimeter in the channel that is in contact with the coolant,

$A = (\pi/4)(0.996)^2 - (0.156)(0.983) = 0.629$ in.,

$P = \pi(0.996) + 2(0.156) + 2(0.983) = 5.413$ in.,

$D_e = \frac{4(0.629)}{12 \times 5.413} = 0.0387$ ft.

Capsule dimensions taken from drawing.[17]

---

[17]C. F. Leitten, Jr., and W. C. Thurber, Phase I – Foreign Reactor Fuel Sample Irradiation of a U-Si-Al Alloy, Irradiation Request ORNL-MTR-35, ORNL-CF-58-2-109 (Rev) (Oct. 13, 1958) p. 3.

Evaluating the heat-transfer coefficient at this temperature yielded $h = 2260$ Btu $hr^{-1}ft^{-2}{}^{\circ}F^{-1}$. The check calculation is as follows:

for $T_1 = 137^{\circ}F$

$$h\left(\frac{0.0387}{0.3815}\right) = 0.023\left[\frac{(0.0387)(8.7)(61.4)}{3.16 \times 10^{-4}}\right]^{0.8}\left[\frac{(0.996)(1.14)}{0.3815}\right]^{0.3} \quad ;$$

$$h = (0.225)(6.62 \times 10^{4})^{0.8}(2.98)^{0.3} \quad ;$$

$$h = 2260 \text{ Btu hr}^{-1}\text{ft}^{-2}{}^{\circ}\text{F}^{-1} \quad ;$$

then from equation (1):

$$\frac{Q}{A_s} = h(T_1 - T_0) \quad ;$$

$$\frac{4.10 \times 10^{3}}{0.0819} = (2260)(T_1 - 115) \quad ;$$

$$T_1 = \frac{5.01 \times 10^{4} + 2260(115)}{2260} \quad ;$$

$$T_1 \cong 137^{\circ}F \quad .$$

<u>The Heat Output in Watts per Inch</u>

The heat output can be obtained as follows:

$$\frac{1.2 \times 10^{3} \text{ w}}{6 \text{ in.}} = 2 \times 10^{2} \text{ w/in.}$$

Appendix B

Irradiation History

Appendix B

Irradiation History of ORNL-MTR-39 Eu_2O_3–Stainless Steel Absorber Specimens

Specimen	Eu_2O_3 Loading (wt %)	Inclusive ETR Irradiation Cycles	Thermal Neutron Flux[a] (neutrons $cm^{-2}sec^{-1}$)	Irradiation Period[b]	Specimen Dose[a] (neutrons/ cm^2)
			$\times 10^{14}$		$\times 10^{20}$
39-1	20	24–28	1.0	82	7.0
39-2	20	24–30	1.2	113	12.1
39-3	20	24–42	1.0	329	28.4
39-4	20	24–46	1.2	422	45.0
39-5	30	24–28	1.5	58	7.6
39-6	30	24–31	1.4	121	14.6
39-7	30	24–40	1.2	281	27.9
39-8	30	24–46	1.2	422	45.0
39-9	40	24–28	1.0	82	7.2
39-10	40	24–33	1.0	171	14.8
39-11	40	24–40	1.2	281	28.7
39-12	40	24–49	1.0	475	42.8

[a]Based upon ETR-quoted unperturbed thermal-neutron fluxes.

[b]Effective full-power days of reactor operation.

Appendix C

Calculation of Europium Depletion

Method of Calculating Europium Depletion from Isotopic Analysis Data

Natural europium consists of 47.8 at. % ^{151}Eu and 52.2 at. % ^{153}Eu. As shown in Fig. 12, three additional highly absorbing product isotopes are produced by neutron capture during irradiation. A neutron absorption in ^{151}Eu may result in either of two isomers of ^{152}Eu. About 16.3% of the captures produce a short-lived isomer (^{152a}Eu), which decays to a stable low-cross-section isotope of gadolinium (^{152}Gd). The remaining 83.7% of the captures form the high-cross-section isotope ^{152b}Eu. Subsequent neutron absorptions progressively result in the formation of ^{153}Eu, ^{154}Eu, ^{155}Eu, and ^{156}Eu. Beta decay of the radioactive isotopes ^{152b}Eu, ^{154}Eu, ^{155}Eu, and ^{156}Eu result in the formation of stable gadolinium isotopes ^{152}Gd, ^{154}Gd, ^{155}Gd, and ^{156}Gd; only one of which (^{155}Gd) has a significant absorption cross section.

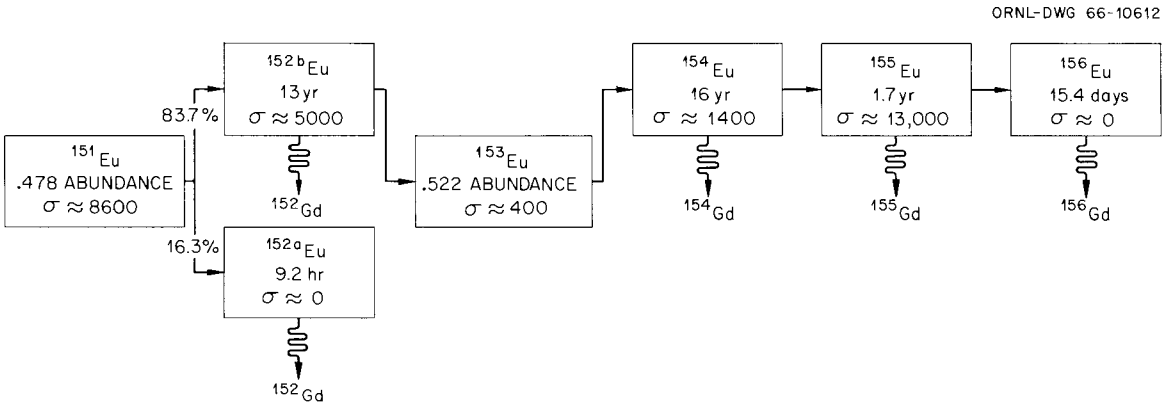

Fig. 12. Europium Burnup Chain.

We see from this discussion that neutron irradiation of natural europium results predominately in the formation of europium and gadolinium isotopes whose average mass number is greater than that of natural europium. Thus, if one could determine the average mass number of the irradiated europium plus gadolinium, one could calculate the number of neutrons that had been absorbed by the europium atoms during irradiation. Unfortunately, such an analysis would be both costly and time consuming, since it would require chemical separation of the radioactive

europium and gadolinium, determination of the europium-to-gadolinium atom ratio, and mass spectrographic analyses of both the europium and gadolinium fractions.

Consideration of the europium burnup chain, however, reveals that only relatively small amounts of gadolinium are produced during irradiation of europium. Most of this gadolinium results from the beta decay of the ^{152a}Eu isotope; the long half-lives and high absorption cross sections of ^{152b}Eu, ^{154}Eu, and ^{155}Eu make it highly improbable that significant amounts of gadolinium will be produced by the decay of these europium isotopes. Thus, even for relatively long irradiation periods, one can consider that irradiation of natural europium results in the formation of europium isotopes of a higher average mass number and a small amount of ^{152}Gd. With such an assumption, a simplified method for calculating europium depletion can be derived, which requires only mass spectrographic analysis of the irradiated europium. The derivation of this formula is presented in the following paragraphs.

Assume that a test specimen contains X atoms of europium before irradiation and Y atoms of europium after irradiation. Isotopically, the atom contents before and after irradiation are as shown below:

Isotope	Number of Atoms of Specific Isotope	
	Preirradiation	Postirradiation
^{151}Eu	a	a′
^{152}Eu		b′
^{153}Eu	c	c′
^{154}Eu		d′
^{155}Eu		e′
^{156}Eu		f′
Total	X	Y

Since we have assumed that ^{152}Gd is the only noneuropium species produced during irradiation, the total number Z of ^{152}Gd atoms produced during irradiation must be

$$Z = X - Y \quad . \tag{1}$$

The number of ^{151}Eu atoms that have absorbed neutrons during irradiation is $a - a'$. Since 16.3% of the neutron absorptions by ^{151}Eu form ^{152a}Eu with subsequent decay to ^{152}Gd,

$$Z = 0.163(a - a') \quad , \tag{2}$$

therefore, equating (1) and (2) gives

$$X - Y = 0.163(a - a') \quad . \tag{3}$$

However, unirradiated natural europium consists of 47.8 at. % ^{151}Eu and 52.2 at. % ^{153}Eu. Therefore, $a = 0.478X$. Since the atom fraction E^{151} of ^{151}Eu in the irradiated europium is determined from mass spectrographic analysis, we can find $a' = E^{151}Y$. By substituting these values for $\underline{a}$ and $\underline{a'}$,

$$X - Y = 0.163(0.478X - E^{151}Y) \quad ; \tag{4}$$

$$Y = 0.9221X/(1 - 0.163\ E^{151}) \quad . \tag{5}$$

Now consider a test specimen that contained 100 atoms of natural europium before irradiation. Postirradiation mass spectrographic analysis reveals that the isotopic composition of the irradiated europium is as follows:

Isotope	Fraction
^{151}Eu	E^{151}
^{152}Eu	E^{152}
^{153}Eu	E^{153}
^{154}Eu	E^{154}
^{155}Eu	E^{155}
^{156}Eu	E^{156}

With Eq. (5) the total number of europium atoms remaining after irradiation can be determined. The total number of atoms of each specific europium isotope is then

$$
\begin{aligned}
{}^{151}Eu &= Y(E^{151}) \\
{}^{152}Eu &= Y(E^{152}) \\
{}^{153}Eu &= Y(E^{153}) \\
{}^{154}Eu &= Y(E^{154}) \\
{}^{155}Eu &= Y(E^{155}) \\
{}^{156}Eu &= Y(E^{156})
\end{aligned}
$$

However, 100 − Y atoms of ^{152}Gd are produced by irradiation. From the standpoint of neutron absorptions, ^{152}Gd can be considered to be equivalent to ^{152}Eu. Thus, the total number of europium and gadolinium atoms of each specific mass number is

Isotope		Number of Atoms of Specific Mass Number	
	^{151}Eu =	$Y(E^{151})$	
^{152}Eu +	^{152}Gd =	$Y(E^{151})$	+ (100-Y)
	^{153}Eu =	$Y(E^{152})$	
	^{154}Eu =	$Y(E^{153})$	
	^{155}Eu =	$Y(E^{154})$	
	^{156}Eu =	$Y(E^{155})$	

The average mass number of the irradiated europium plus gadolinium is then

$$\langle A \rangle = \sum n_1 A_1 \quad , \tag{6}$$

where:

$\langle A \rangle$ = average mass number of irradiated europium plus gadolinium,

n_1 = atom fraction of specific isotope,

A_1 = mass number of specific isotope.

The average mass of unirradiated natural europium is 152.044 based upon a ^{151}Eu atom fraction of 0.478 and a ^{153}Eu atom fraction of 0.522. The change in the average mass number of the europium caused by the absorption of neutrons is, therefore,

$$\Delta A = \langle A \rangle - 152.044 \quad . \tag{7}$$

This change in mass is obviously a result of neutron absorptions by the europium nucleus and, therefore, represents the average number of neutrons absorbed by each original europium atom. The burnup of europium is, therefore, equivalent to ΔA, and Eq. 7 becomes

$$B.U. = \langle A \rangle - 152.044 \quad , \tag{8}$$

where:

B.U. = europium burnup in neutrons absorbed per initial europium atom.

Expressed in terms of neutrons absorbed per cubic centimeter of total core material, Eq. (8) becomes

$$B.U. = (\langle A \rangle - 152.044)N \quad , \tag{9}$$

where

N = number of original europium atoms per cubic centimeter of core.

In our experiments $N = 4.67 \times 10^{21}$, 7.12×10^{21}, and 9.32×10^{21} atom/cm^3 for the 20, 30, and 40 wt % Eu_2O_3–stainless steel mixtures respectively.

To check the results obtained from our "mass difference" method, we also developed another system. Jankowski[18] calculated the variation of the isotopic content of europium as a function of burnup. Using Jankowski's results, we developed a relationship between the ^{151}Eu-to-^{153}Eu ratio and the number of neutrons absorbed per original europium atom, which is shown in Fig. 13. Using the data listed in Table 7, we calculated the ^{151}Eu-to-^{153}Eu ratio for each irradiated specimen and, by referring to Fig. 13, obtained burnup values for each specimen. As shown in the last column of Table 7, burnups obtained by the "mass difference" method agree well with those obtained from the ^{151}Eu-to-^{153}Eu ratio.

---

[18]F. J. Jankowski, "Experimental Determination of Control Rod Worth," pp. 106–09 in Neutron Absorber Materials for Reactor Control, ed. by W. K. Anderson and J. S. Theilacker, Naval Reactors Handbook, 1962.

Table 7. Mass Spectrographic Analyses of Europium Contained in the Irradiation Test Specimens

Specimen	Eu_2O_3 (wt %)	Atom Fraction of Isotope					Average Mass Number of Eu + Gd	Burnup (neutron absorptions/original Eu atom)	
		Eu^{151}	Eu^{152}	Eu^{153}	Eu^{154}	Eu^{155}		By Eu^{151}/Eu^{153} Method	By Mass Difference Method
39-2	20	0.350	0.078	0.555	0.017	0.000	152.235	0.18	0.193
39-3	20	0.150	0.122	0.680	0.048	0.000	152.591	0.54	0.549
39-4	20	0.003	0.173	0.692	0.090	0.042	152.918	1.00	0.876
39-10	40	0.312	0.097	0.568	0.012	0.011	152.306	0.23	0.264
39-11	40	0.218	0.133	0.606	0.025	0.018	152.470	0.39	0.428
39-12	40	0.117	0.103	0.690	0.062	0.028	152.876	0.61	0.691

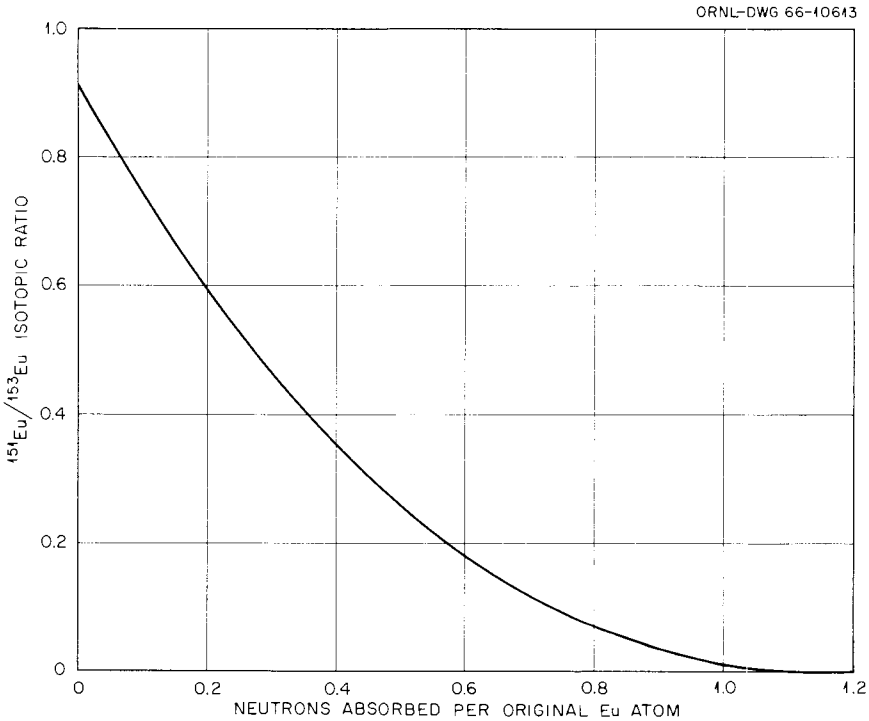

Fig. 13. Variation of the ^{151}Eu-to-^{153}Eu Ratio with Burnup.

Mass spectrographic analyses were obtained on only 6 of the 12 specimens irradiated in the test program. However, burnup values for the other six test specimens were obtained by interpolation of the relationship illustrated in Fig. 14.

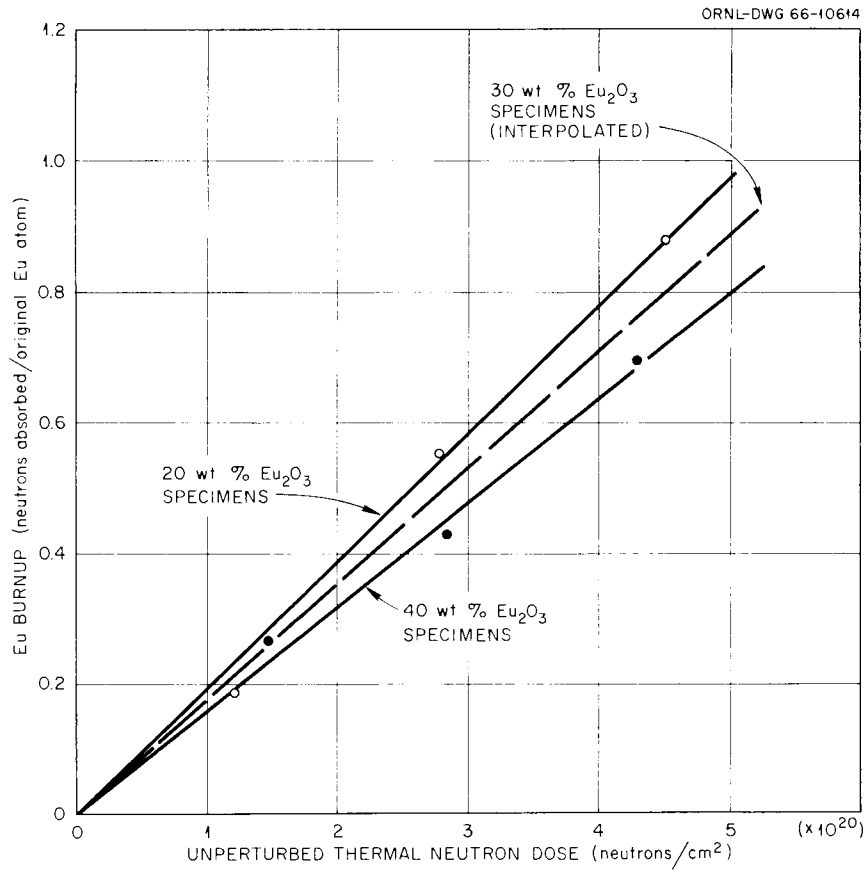

Fig. 14. Burnup vs Exposure for Eu_2O_3–Stainless Steel Irradiation Test Specimens.

ORNL-4104
UC-25 Metals, Ceramics, and Materials

INTERNAL DISTRIBUTION

1–2. Central Research Library
3–4. ORNL – Y-12 Technical Library Document Reference Section
5–24. Laboratory Records Department
25. Laboratory Records, ORNL RC
26. ORNL Patent Office
27. G. M. Adamson, Jr.
28. R. J. Beaver
29. A. L. Boch
30. G. E. Boyd
31. G. L. Copeland
32. F. L. Culler
33. J. E. Cunningham
34. J. H Frye, Jr.
35. R. E. Gehlbach
36. R. J. Gray
37. V. O. Haynes
38–40. M. R. Hill
41. G. W. Keilholtz
42. R. T. King
43. C. E. Larson
44–48. C. F. Leitten, Jr.
49. R. E. Lewis
50. M. M. Martin
51. W. R. Martin
52. H. G. MacPherson
53. H. C. McCurdy
54. D. L. McElroy
55. S. Peterson
56. A. E. Richt
57. C. E. Sessions
58. T. N. Washburn
59. A. M. Weinberg
60. M. L. Winton
61. M. B. Bever (consultant)
62. A. R. Kaufmann (consultant)
63. J. A. Krumhansl (consultant)

EXTERNAL DISTRIBUTION

64. V. P. Calkins, General Electric, NMPO
65. W. Cashin, Knolls Atomic Power Laboratory
66. S. Christopher, Combustion Engineering, Inc.
67. D. B. Coburn, General Atomic
68. D. F. Cope, RDT, OSR, AEC, Oak Ridge National Laboratory
69. G. K. Dicker, Division of Reactor Development and Technology, AEC, Washington
70. D. E. Erb, Division of Reactor Development and Technology, AEC, Washington
71. E. A. Evans, General Electric, Vallecitos
72. W. C. Francis, Idaho Nuclear Corporation
73. A. J. Goodjohn, General Atomic
74. J. L. Gregg, Bard Hall, Cornell University
75. R. G. Grove, Mound Laboratory
76. D. H. Gurinsky, Brookhaven National Laboratory
77. A. N. Holden, General Electric, ADED
78–80. J. S. Kane, Lawrence Radiation Laboratory, Livermore
81. H. Kato, U.S. Department of the Interior, Bureau of Mines
82. J. H. Kittel, Argonne National Laboratory
83. E. J. Kreih, Westinghouse, Bettis Atomic Power Laboratory
84. W. J. Larkin, AEC, Oak Ridge Operations

85. W. L. Larsen, Iowa State University, Ames Laboratory
86. J. J. Lombardo, NASA, Lewis Research Center
87. J. H. MacMillan, Babcock and Wilcox Company
88. R. Mayfield, Argonne National Laboratory
89. M. McGurty, General Electric, NMPO
90. M. Nevitt, Argonne National Laboratory
91. R. E. Pahler, Division of Reactor Development and Technology, AEC, Washington
92. S. Paprocki, Battelle Memorial Institute
93. D. Ragone, General Atomic
94. B. Rubin, Lawrence Radiation Laboratory, Livermore
95. F. C. Schwenk, Division of Reactor Development and Technology, AEC, Washington
96–98. J. M. Simmons, Division of Reactor Development and Technology, AEC, Washington
99. L. E. Steele, Naval Research Laboratory
100. R. H. Steele, Division of Reactor Development and Technology, AEC, Washington
101. W. F. Sheely, Division of Research, AEC, Washington
102. E. E. Stansbury, the University of Tennessee
103. D. K. Stevens, Division of Research, AEC, Washington
104. A. Strasser, United Nuclear Corporation
105. A. Taboada, Division of Reactor Development and Technology, AEC, Washington
106. A. Van Echo, Division of Reactor Development and Technology, AEC, Washington
107. R. Van Tyne, Illinois Institute of Technology Research Institute
108. C. E. Weber, Atomics International
109. G. W. Wensch, Division of Reactor Development and Technology, AEC, Washington
110. Division of Research and Development, AEC, Oak Ridge Operations
111–382. Given distribution as shown in TID-4500 under Metals, Ceramics, and Materials category (25 copies — CFSTI)